SPE-190179-MS

Improving CO_2 Foam for EOR Applications Using Polyelectrolyte Complex Nanoparticles Tolerant of High Salinity Produced Water

Negar Nazari, Jyung-Syung Tsau, Reza Barati, University of Kansas

This paper was prepared for presentation at the SPE Improved Oil Recovery Conference held in Tulsa, Oklahoma, USA, 14-18 April 2018.

Abstract

Although surfactant generated CO_2 foam improves the mobility control for CO_2 flooding, it suffers from instability in the presence of crude oil and in high salinity environments. The objective of this work is to improve the stability of the interface by lowering surfactant drainage and improving the stability of lamellae in high salinity produced water using polyelectrolyte complex nanoparticles and generate a more stable foam front in the presence of crude oil. This results in improving the recovery efficiency of foam floods.

In this project, an optimized system of polyelectrolyte complex nanoparticles was used to improve $scCO_2$ foams prepared in high salinity produced water. The effect of nanoparticles on the interfacial properties of the foam was studied. Thereafter, a set of core flooding experiments with and without the crude oil in the system was conducted to measure the apparent viscosity and the incremental oil recovery due to addition of polyelectrolyte and polyelectrolyte complex nanoparticles to the surfactant generated CO_2 foam in high salinity produced water.

Studying the interfacial properties of different foam systems shows that addition of polyelectrolytes and polyelectrolyte complex nanoparticles to the surfactant generated CO_2 foam improves the elasticity of the interface. Furthermore, adding polyelectrolytes and polyelectrolyte complex nanoparticles to the surfactant generated CO_2 foam, improves the efficiency of the oil recovery by improving the apparent viscosity and making the foam more stable in the presence of crude oil. Polyelectrolyte complex nanoparticles produced incremental oil when the surfactant foam system reached its residual oil and produced no more oil.

Generating a very stable system of the foam by adding polyelectrolyte complex nanoparticles to the surfactant generated CO_2 foam prepared in high salinity produced water, results in a longer lasting foam and increase the incremental oil recovery up to 10%. The sea water salinity is applicable for all the locations with access to the sea water as well as locations with produced water salinities close to sea water. The higher salinity system covers a wide range of the reservoirs in the United States and worldwide with access to produced water.

Introduction

CO_2 has been used as an enhanced oil recovery (EOR) technique since 1950s (Langston, et al., 1988). But it suffers from unfavorable mobility ratio, viscous fingering, gravity override and poor sweep efficiency. Therefore, several methods have been implemented to improve the application of CO_2 for EOR applications (Green & Willhite, 1998). The alternate injection of water with CO_2 was used to combat this problem and has been tested for different fields (Barati, et al., 2016; Caudle & Dyes, 1958), but due to the comparability of water viscosity with the viscosity of supercritical CO_2 at reservoir temperature, the mobility ratio improvement was not significant in some cases.

CO_2 foam, as an effective mobility control agent, was initially presented by Bernard and Holm (Bernard & Holm, 1967) to improve the sweep efficiency of the EOR processes (JPT, 1998; Fried, 1961). Foam is a special colloidal dispersion that consists of a gas, a liquid and a foaming agent (Lord, 1981). Due to the spreading of the oil on the foam lamellae, the stability of the surfactant generated CO_2 foam in the presence of crude oil is very crucial. In addition, the oil adsorption by the porous media hardens the foam generation and degeneration by altering the wettability of the rock (Schramm, 1994).

Kalyanaraman et al. (Kalyanaraman, et al., 2016) developed a system of nanoparticles for stabilizing the CO_2 foam in the presence of crude oil. Their developed system, had the capability of making foams more stable in 2% KCl brine and results in increasing the oil recovery and sweep efficiency of the reservoir.

Large volumes of produced water from oil fields is a very important concern for the oil industry (Patel, et al., 2004). Disposal, treatment and re-use of the produced water are the available methods to handle the oil field produced water (Evans & Robinson, 1999). Water disposal is controlled by the environmental regulations. Since handling and treatment of the produced water increases operational costs and requires costly infrastructure, re-injecting the produced water into the reservoir for EOR applications is the most optimized method to handle the produced water (Caudle, 2002). Re-injection of the produced water for enhanced oil recovery applications reduces the treatment difficulties while lowering the usage of fresh water in the oil industry (Nazari, et al., 2017).

The main objective of this research is to stabilize the surfactant generated CO_2 foam using polyelectrolyte complex nanoparticles (PECNP) in high salinity produced water and in the presence of crude oil. Forming the polyelectrolyte/surfactant complexes in oppositely charged systems of surfactant and polyelectrolyte, stabilizes the foam film by decreasing the surface elasticity (Kristen & Klitzing, 2009). In this work, the PECNP systems developed by Nazari et al. (Nazari, et al., 2017) was used to analyze the effect of nanoparticles on interfacial tension and incremental oil recovery.

Materials

Polyethyleneimine

Polyethyleneimine (PEI), which comes in two forms of linear and branched, is a polymer formed from repeating unit composed of an amine group and a two-carbon aliphatic CH_2CH_2 spacer (Yemul & Imae, June 2008). The branched PEI with a molecular weight of 25 kDa, reported by Sigma Aldrich, St. Louis, MO, USA (CAS# 9002-98-6), was used in this study. The density and viscosity of the used PEI is 1.03 g/ml and 13,000-18,000 cP at 25 and 50 degrees Celsius, respectively. The chemical structure of the intended branched PEI is shown in Figure 1.

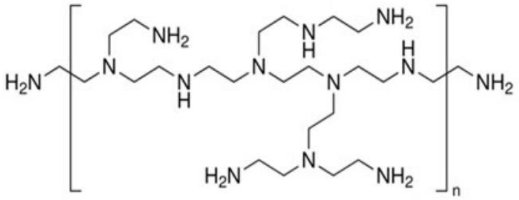

Figure 1. The Polyethyleneimine chemical structure *(Barati, 2010)*.

Dextran Sulfate

Dextran Sulfate sodium salt (DS) is a polyanion in powder form. The sulfur content and average molecular weight of this product is between 17 to 20% and 500,000, respectively. It was purchased from Fisher Chemical, St. Louis, MO, USA (CAS# 9011-18-1). The chemical structure of DS monomer is shown in Figure 2.

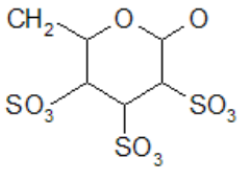

Figure 2. The Dextran Sulfate chemical structure *(Barati, 2010)*.

Surfactant

SURFONIC N-120 surfactant, with an anionic nature and 12 Ethylene oxide (EO) groups, is a surface-active agent compatible with other nonionic surfactants and with most anionic and cationic surfactants. The theoretical molecular weight and hydroxyl number of this surfactant is 748 and 75, respectively. The density of this product is 1.066 g/mL at 25 degrees Celsius. This surfactant was provided by Huntsman Chemicals, Woodlands, TX, USA (CAS# 9016-45-9).

Mississippian Limestone Brine

The formulation of a brine from the Mississippian Limestone Play (MLP) brine sample was prepared in Reverse Osmosis (RO)-Deionized (DI) water as a synthetic solution. The composition and related information of the salts in the brine is shown in Table 1. In order to prepare the salinity of 33,667 ppm and 67,333 ppm, the MLP brine was diluted 6 and 3 times using DI-RO water, respectively.

Table 1. The final composition of the MLP brine.

Brine Composition	Concentration (mg/L)	Provider	CAS #	Location
NaCl	163661.82	Fisher Chemical	7647-14-5	Lenexa, KS
Na_2SO_4	1224.3	Fisher Chemical	7757-82-6	
KCl	714.93	AMRESCO	7447-40-7	Solon, OH
$MgCl_2.6H_2O$	21759.36	Fisher Chemical	7791-18-6	
$CaCl_2.2H_2O$	46886.13	Fisher Chemical	10035-04-8	
$SrCl_2.6H_2O$	1535.60	Fisher Chemical	10025-70-4	
Total	235782.11			

Crude Oil

Mississippian crude oil, with the asphaltenes content of 0.5 wt%, is used for core flooding experiments. The viscosity and density were measured to be 3.88 cP and 0.82 g/cc, respectively, at 40 degrees Celsius.

Cores

The Indiana limestone outcrops with the reported permeability of 135 mD were used for core flooding experiments. The diameter and the length of the used cores were 1.5 inches and 9 inches, respectively. The detailed properties of the cores, used in this study, are reported in the Results and Discussion section.

Samples Preparation

Surfactant Solutions

The surfactant solution was prepared in two different salinities of 33,667 and 67,333 ppm. It was stirred for 30 minutes at 500 revolutions per minute (rpm). The final concentration of the surfactant in the solutions was kept at 0.1 wt% for all the systems.

Polyethyleneimine Solution

The PEI solution was prepared in two different salinities of 33,667 and 67,333 ppm. Solutions were stirred for 30 minutes at 500 rpm. The concentration of the PEI in the solutions was 1 wt%. The pH of the 600 ml of 1 wt% PEI solution was measured to be 10.45±0.18 for two different salinities of 33,667 and 67,333 ppm. The pH was lowered to 8 by adding 5.5 mL of 12N Hydrochloric acid (HCl) to the PEI solution in both salinities.

Dextran Sulfate Solution

The DS solution was prepared in two different salinities of 33,667 and 67,333 ppm. Solutions were stirred for 30 minutes at 500 rpm. The concentration of the DS in both brines was 1 wt%.

Nanoparticle Solutions

For preparing the polyelectrolyte complex nanoparticle (PECNP) systems, different combinations of PEI: DS were prepared in two different salinities of 33,667 and 67,333 ppm salinities of diluted MLP brine and in original salinity of 202,000 ppm. The most optimized ratio of PEI: DS was selected for each salinity based on the zeta potential and particle size measurements which were presented by Nazari et al (Nazari, et al., 2017). In this study four different PEI to DS ratios of 1, 2, 3 and 4 have been prepared. For the ratios of 1: 1 and 2: 1 for PEI: DS, the precipitation occurred and they were removed from our studies. Among the ratios of 3: 1 and 4: 1, the ratio of 3: 1: 0.1 of PEI: DS: brine was selected based on our particle size and zeta potential measurements (Nazari, et al., 2017). The sample was stirred for 30 minutes at 500 rpm. The nanoparticle solutions were prepared in the brine of up to 200,000 ppm salinity and they were stable in two ratios of 3: 1: 0.1 and 4: 1: 0.1 for PEI: DS: brine. The limiting factor for the experiments was the surfactant. Different ratios of PEI over DS and PECNP over surfactant solution in different pH of PEI, which has been considered to prepare the PECNP synthesis are shown in Table 2.

Table 2. Summary of PEI: DS and PECNP: surfactant ratios along with the different pH of PEI used for preparation of the PECNP batch for initial screening.

Batch #	pH (of PEI)	Final pH (33,667 ppm)	Final pH (67,333 ppm)	Ratio (PEI: DS: MLP brine)	Ratio (PECNP: Surfactant)
1	8.00	7.91	8.08	3: 1: 0.1	1: 9
2	8.00	7.93	8.18	3: 1: 0.1	2: 8
3	8.00	7.94	8.12	3: 1: 0.1	3: 7
4	8.00	7.94	8.15	3: 1: 0.1	4: 6
5	8.00	7.90	8.25	3: 1: 0.1	5: 5
6	8.00	7.85	8.01	4: 1: 0.1	1: 9
7	8.00	7.92	8.21	4: 1: 0.1	2: 8
8	8.00	7.96	8.15	4: 1: 0.1	3: 7
9	8.00	7.97	8.15	4: 1: 0.1	4: 6
10	8.00	8.00	8.27	4: 1: 0.1	5: 5

PEI-Surfactant and PECNP-Surfactant Systems

After preparing the surfactant solution and the nanoparticle solution in any specific brine, the PEI: Surfactant and the PECNP: Surfactant systems in two ratios of 1: 9 and 2: 8 were chosen for two different salinities of 33,667 and 67,333 ppm, respectively. Then, the solutions were stirred for 30 minutes at 500 rpm. The final pH of the solution depends on the pH of the PEI which was used for preparing the sample,

but the final concentration of the surfactant in the solutions was kept at 0.1 wt% by adjusting the concentration of the surfactant stock solutions.

Methods and Experimental Setups

Interfacial Tension Measurements

Interfacial tension (IFT) is the surface tension exerted to the interface of two immiscible fluids (Nazari, et al., 2017). Decreasing the interfacial tension results into decreasing the capillary forces between the oil and the brine and enhancing the oil recovery (Xu, 2005). For the purpose of this study, an IFT setup by Core Laboratories Inc. is modified to analyze the effect of nanoparticles on the interfacial properties using the pendant drop method for foam systems. Figure 3 shows the schematic diagram of the modified IFT setup.

This setup includes a chamber which is used to contain the aqueous phase. The cylindrical accumulator is used to inject the aqueous phase into the system. An ISCO pump is used to inject the air or the CO_2 phase. The densities of two phases are entered as inputs into the software. A camera is installed in front of the chamber to take photos from the pendant bubble staying on the needle. The photos taken by camera are sent to the Drop-image software to calculate the interfacial tension. The interfacial tension between supercritical CO_2 and different aqueous phases (surfactant, PEI-surfactant, and PECNP-surfactant) are measured at the pressure and the temperature of 1350 psi and 40 degrees Celsius, respectively.

The dynamic IFT measurements for the supercritical CO_2 tests is conducted for 1200 points in 1 second intervals for a total time of 20 minutes.

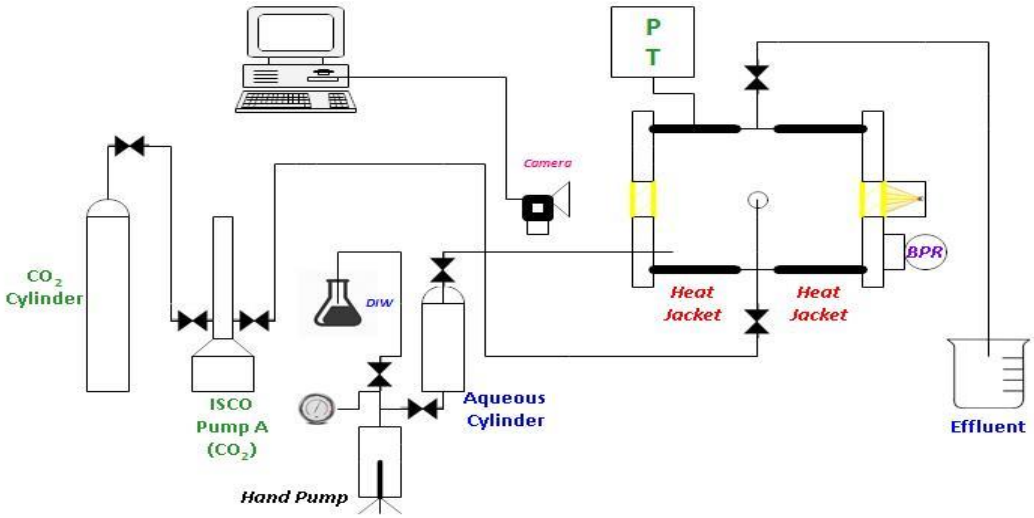

Figure 3. Schematic diagram of the interfacial tension setup.

Dilatational Elasticity

The dynamic behavior of IFT is as important as the static behavior in enhanced oil recovery applications. However, the studies of dynamic behavior of IFT has been largely ignored in the existing literature due to experimental complexities (Boury, et al., 1995; Tewes, et al., 2011). The dilatational elasticity of the surface is calculated by conducting the dynamic IFT measurements. In calculating the dilatational elasticity, Figure 4 is considered:

The total surface pressure change is considered as:

$$\Delta\pi = \Delta\pi_e + \Delta\pi_{ne} \quad \text{(Equation 1)}$$

where $\Delta\pi_e$ represent changes in surface pressure of the equilibrium part of the curve which can be expressed as:

$$\Delta\pi_e = E_e \frac{U_b t}{A_i} \quad \text{(Equation 2)}$$

where A_i is the initial surface area.
Equation 2 is written as:

$$\Delta\pi_e = E_e \frac{\Delta A}{A_i} \quad \text{(Equation 3)}$$

From Equation 3, Ee, which is the equilibrium surface dilatational elasticity, is calculated. The $\Delta\pi_e$'s values and the surface areas size of droplet developed are known from IFT measurement.

To determine the nonequilibrium surface dilatational elasticity, E_{ne}, the equation below can be applied:

$$\Delta\pi_{ne} = \frac{E_{ne} U_b t}{A_i}\left(1 - e^{-t/\tau}\right) \quad \text{(Equation 4)}$$

where $-t/\tau$ is the relative relaxation, which is calculated by assuming that the time of compression, t, that is the time used to generate the initial droplet, is much smaller than the time of relaxation, τ, that is the time taken for the developed droplet to break off. In our dynamic IFT measurement, the condition is fulfilled. Therefore, the equation below can be used to calculate $-t/\tau$:

$$-\frac{t}{\tau} = ln\frac{\pi_{(t)} - \pi_\infty}{\pi_0 - \pi_\infty} \quad \text{(Equation 5)}$$

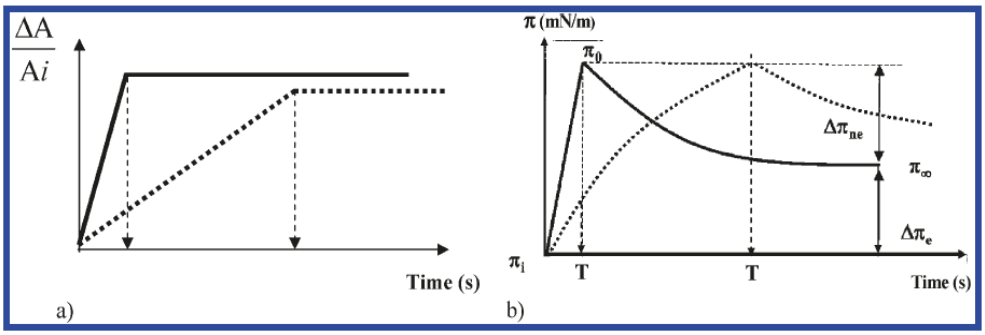

Figure 4. (a) Relative area compression and (b) surface pressure variation Δπ over time T *(Tewes, et al., 2011)*.

Core Flooding by CO_2 Foam

Porosity and Permeability Measurement

The core flooding experiments are conducted to measure the incremental oil recovery. The schematic diagram of the core flooding setup is shown in Figure 5. In order to mimic the reservoir conditions, the core sample is fully saturated with desired brine sample. The 12-inch long, 1.5-inch diameter Indiana limestone cores were used for this experiment. The cores are cut into the desired length of 9 inches and placed in the oven for 24 hours at 75-80 degrees Celsius. The weight of the cores is measured with time till no more changes is observed. The final weight of the dry core is written and the core is placed in the core holder. The overburden pressure of 1000 psi is applied on the core and the core is vacuumed using a vacuum pump till a pressure reading of -28 to -30 psi is achieved. Thereafter, the core is saturated with desired brine. After saturating the core, it is removed from the core holder. The saturated weight of the core is measured to calculate the pore volume (PV) and the porosity of the core. The pore volume and porosity of the core can be calculated by:

$$PV = \frac{(Weight\ of\ the\ saturated\ core - Weight\ of\ the\ dry\ core)}{Brine\ Density} \quad \text{(Equation 6)}$$

$$Porosity\ (\varphi) = \frac{PV}{Bulk\ Volume} \quad \text{(Equation 7)}$$

After porosity measurement, the saturated core is placed in the core holder again to measure the permeability. The pressure and the temperature of the setup is set to be 1350 psi and 40 degrees Celsius, respectively. Simultaneously, the overburden pressure is increased gradually in the steps of 100 psi to the desired value of 1850-1900 psi. The brine is flowed through the core holder in 3 different flow rates. The pressure drops across the core due to each flow rate are monitored using the Validyne transducer #4. The schematic diagram of the flow path for permeability measurement is shown in Figure 6. The core permeability is calculated by substituting the different flow rates and pressure drops in Darcy's equation considering the sizes of the core and the viscosity of the used brine:

$$Q = \left(\frac{k*A}{\mu*L}\right) * \Delta P \quad \text{(Equation 8)}$$

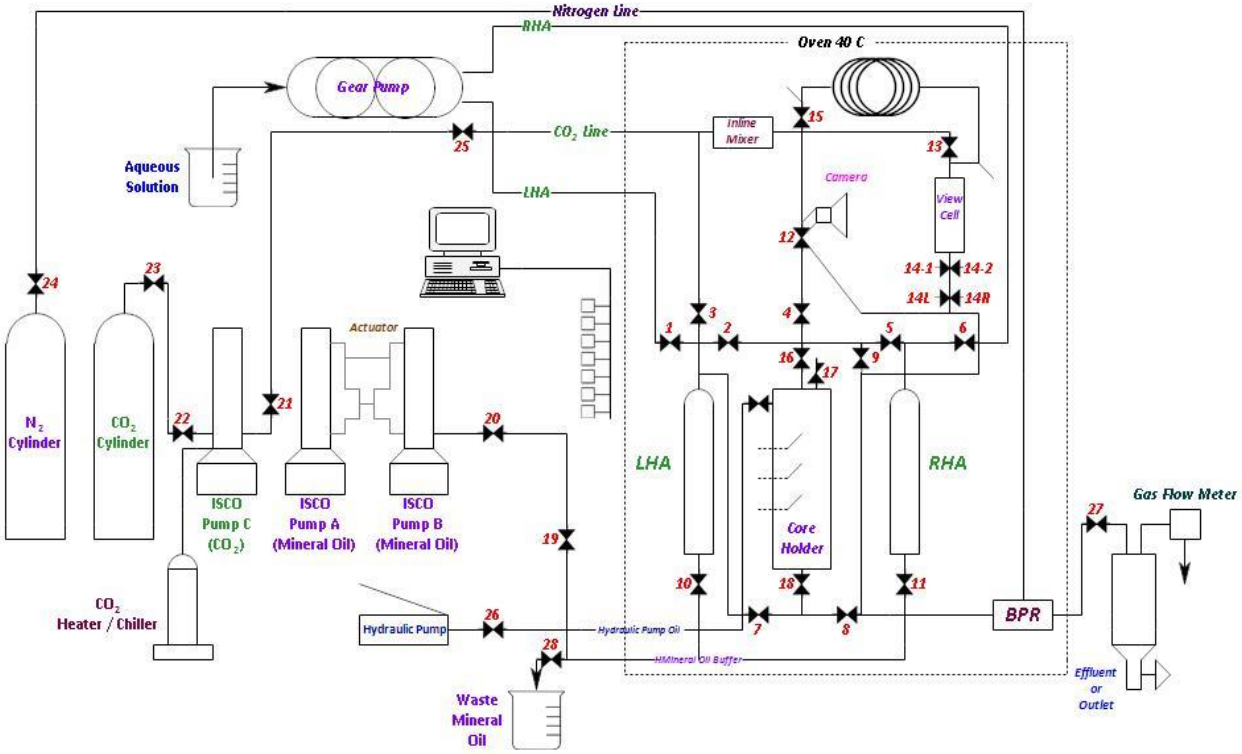

Figure 5. Schematic diagram of the core-flooding setup.

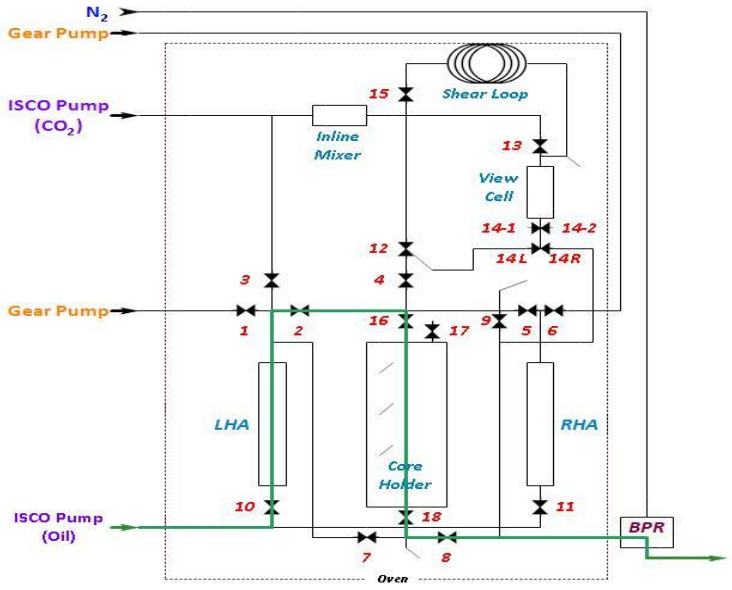

Figure 6. Schematic diagram of the flow paths to inject any aqueous phase through the core. This flow path is used during the permeability measurement, surfactant injection, PEI-surfactant injection, PECNP-injection, and waterflooding.

ScCO$_2$ Foam Flooding Without Crude Oil in the System

The foam is composed of the desired aqueous phase and the supercritical CO_2. The pump C in Figure 5 is used to keep the CO_2 and pumps A and B are used to inject the Soltrol into the transfer cylinder to inject the aqueous phase. Once the pump is filled with CO_2, to maintain CO_2 in supercritical state, the temperature of the heater is adjusted to 40 degrees Celsius. The pressure of 1350 psi is desired for this experiment. For starting the foam injection, considering the quality of the foam (90% for the purpose of this study) the flow rate of pump C and pumps A and B are adjusted. For this test, the total flow rate of 3 mL/min was conducted. Therefore, the flow rate of pump C is adjusted to 2.7 mL/min and the flow rate of pumps A and B (acts as one pump) is adjusted to 0.3 mL/min. The foam is pre-generated before injecting into the core by simultaneous passing of the aqueous phase and the supercritical CO_2 through a 7-microns inline filter. Then the foam is flowed through the core. The schematic diagram of the flow paths for the foam injection is presented in Figure 7. The volume of the supercritical CO_2 used for one test is 103 mL and considering the quality of the foam, which is 90%, the aqueous phase volume for each test is 11.4 mL. Therefore, a total of 114.4 mL of foam is injected through the core and the pressure drops are recorded while injecting the foam into the core.

After the foam injection, 6 PVs of the brine is injected through the core, with the flow rate of 3 mL/min, and the permeability of the core is measured again to evaluate the extent of the damage to the core. In total, 6 experiments are conducted without any crude oil in the system using 6 different cores. Three different systems of surfactant generated CO_2 foam, PEI-surfactant generated CO_2 foam, and PECNP-surfactant generated CO_2 foam were tested in two different diluted MLP brine salinities of 33,667 and 67,333 ppm, respectively.

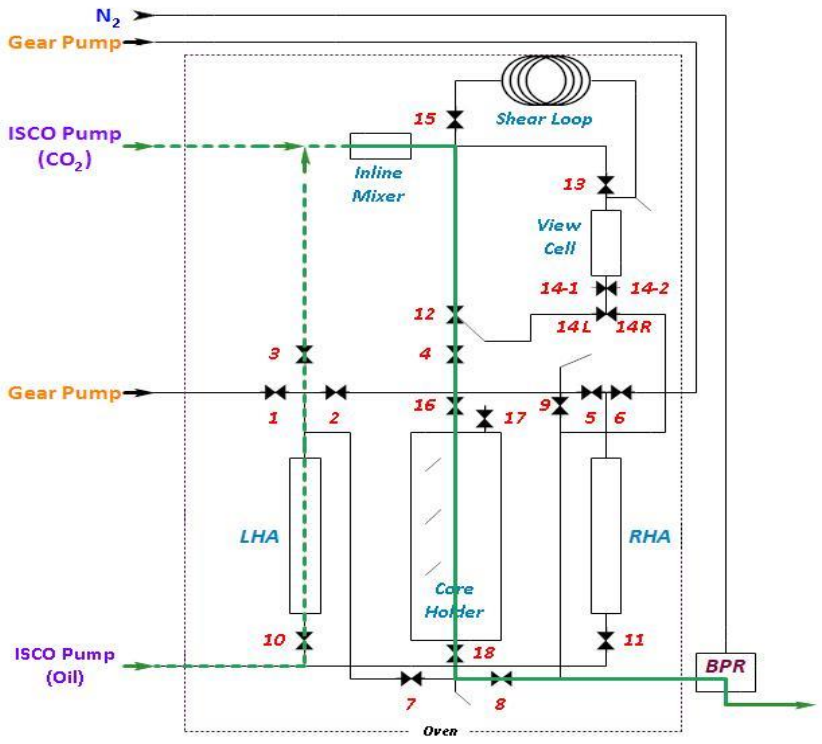

Figure 7. Schematic diagram of the flow paths for the foam flooding.

Core Flooding by CO_2 Foam in the Presence of Crude Oil in the system

After saturating the core and measuring the permeability, primary drainage is started. For this purpose, the oil is injected into the core with the flow rate of 0.5 mL/min till no more water is produced in the outlet. For the purpose of this study, 4 PVs of oil is injected into the core. The pressure and the temperature of the system is maintained at 1350 psi and 40 degrees Celsius, respectively. The volume of the collected water in the outlet is noted down and used for calculating the original oil in place (OOIP) and the initial oil saturation (S_o).

$$OOIP = (Injected\ oil - produced\ oil)\ at\ the\ end\ of\ primary\ drainage \quad \text{(Equation 9)}$$

$$S_o = \frac{OOIP}{PV} \quad \text{(Equation 10)}$$

After primary drainage, the brine is injected into the oil saturated core with the flow rate of 0.5 mL/min. The brine injection is continued till no more oil is produced in the outlet. The water flooding is continued up to 4 PVs for this study. The recovery efficiency of the water flooding process, the residual oil after water flooding and the residual oil saturation (S_{or}) are calculated considering the amount of the produced oil at the end of the water flooding process.

$$Waterflooding\ efficiency\ (\%) = \left(\frac{Produced\ oil\ at\ the\ end\ of\ water\ flooding}{OOIP}\right) * 100 \quad \text{(Equation 11)}$$

$$Residual\ oil\ after\ water\ flooding = OOIP - Produced\ oil\ during\ water\ flooding \quad \text{(Equation 12)}$$

$$S_{or} = \frac{\text{(Residual oil volume after water flooding)}}{\text{PV}} \quad \text{(Equation 13)}$$

After finishing the water flooding, the brine inside the left-hand accumulator is replaced by the desired aqueous phase for the CO_2 foam generation. The accumulator is pressurized and is opened to the system. Simultaneous injection of the supercritical CO_2 and the aqueous phase through a 7-microns inline filter results in generating the foam. The pre-generated foam is diverted into the core and displaces the oil in place. The total flow rate of the foam injection is 3 mL/min and the foam quality is 90%. Three different systems of foam, including surfactant generated CO_2 foam, PEI-surfactant generated CO_2 foam, and PECNP-surfactant generated CO_2 foam are injected through different cores in different orders. The recovery efficiency of each flood is calculated and the residual oil saturation after each system of the foam flooding is calculated. The schematic diagram of the foam flooding is shown in Figure 7.

Finally, the left-hand side (LHA) accumulator is filled with the desired brine and the core is flooded up to 5 PVs.

Results and Discussion

The density and viscosity of the different solutions used in this study are measured and the values are reported in Table 3.

Table 3. Summary of the density and viscosity values measured at the temperature of 40 degrees Celsius for different samples used in this study.

Sample	Pressure (psi)	Density (g/cc)	Viscosity (cP)
DI water	Ambient	0.9920	0.650
6 times diluted MLP brine (33,667 ppm salinity)	Ambient	1.0180	0.750
Surfactant in 33,667 ppm salinity of diluted MLP brine	Ambient	1.0182	0.720
PEI-surfactant in 33,667 ppm salinity of diluted MLP brine	Ambient	1.0186	0.720
PECNP-surfactant in 33,667 ppm salinity of diluted MLP brine	Ambient	1.0185	0.730
3 times diluted MLP brine (67,333 ppm salinity)	Ambient	1.0440	0.800
Surfactant in 67,333 ppm salinity of diluted MLP brine	Ambient	1.0448	0.780
PEI-surfactant in 67,333 ppm salinity of diluted MLP brine	Ambient	1.0456	0.810
PECNP-surfactant in 33,667 ppm salinity of diluted MLP brine	Ambient	1.0456	0.820
Supercritical CO_2	1350	0.5526	0.040
Mississippian crude oil	Ambient	0.8200	3.880

Interfacial Tension Measurements

The interfacial tension between supercritical CO_2 ($scCO_2$) and the aqueous phase (surfactant, PEI-surfactant or PECNP-surfactant) was measured. Figure 8 and Figure 9 show the comparison of the interfacial tension values between a supercritical CO_2 bubble and different aqueous solutions prepared in 6 and 3 times diluted MLP brine. The obtained results confirm that increasing the salinity results in increasing the interfacial tension, thereby destabilizing the foam by screening of the double layer in the foam film in accordance to the DLVO theory (Micheau, et al., June 2013; Sedev & Exerowa, 1999). In contrast, adding polyelectrolytes and polyelectrolyte complex nanoparticles to the surfactant solution results in decreasing the interfacial tension. IFT reduction results in decreasing the capillary forces and thereby lowering the mechanical energy needed to move the foam in the small pores. This will result into improving the recovery effieciency.

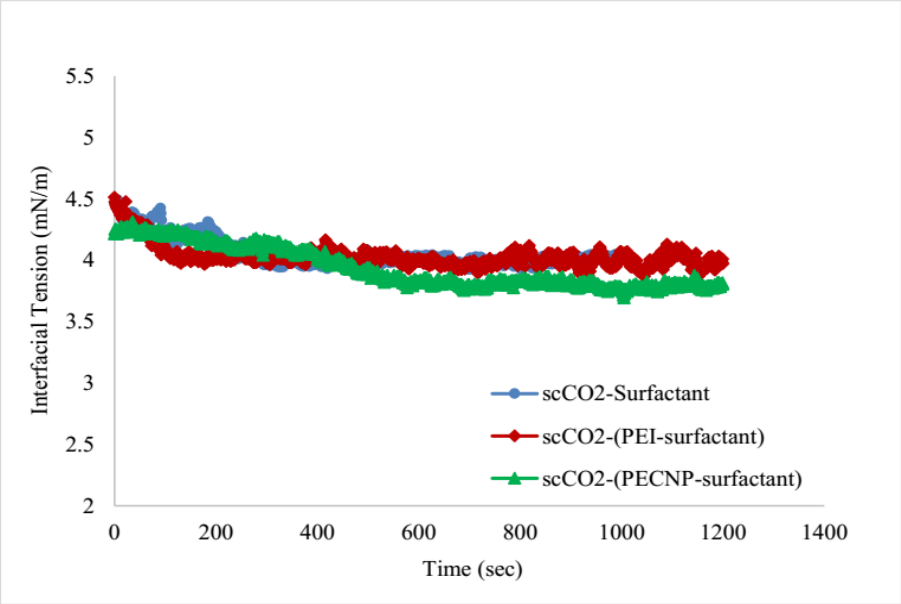

Figure 8. Comparison of the interfacial tension versus time between a supercritical CO_2 bubble and surfactant, PEI-surfactant, and PECNP-surfactant solutions prepared in 33,667 ppm salinity of diluted MLP brine.

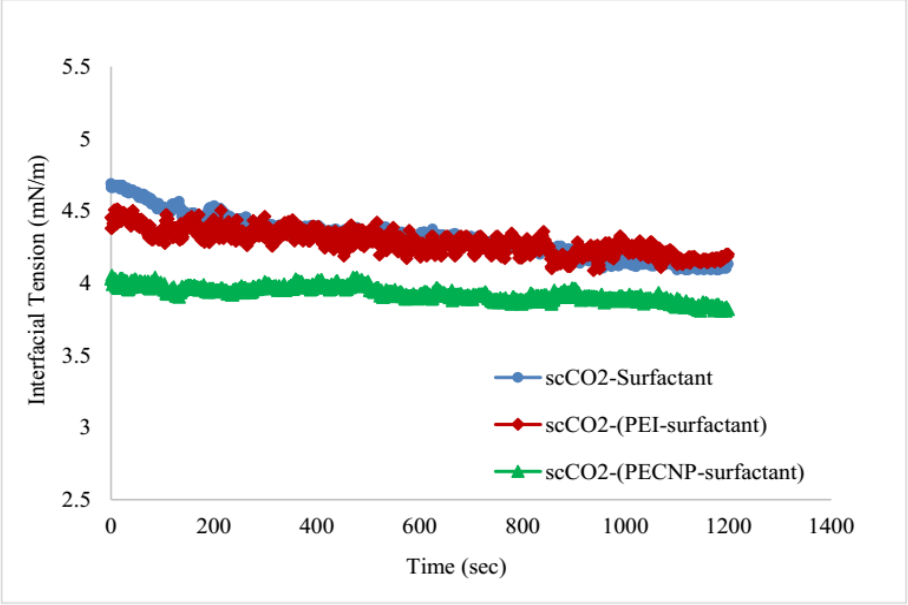

Figure 9. Comparison of the interfacial tension versus time between a supercritical CO_2 bubble and surfactant, PEI-surfactant, and PECNP-surfactant solutions prepared in 67,333 ppm salinity of diluted MLP brine.

Elasticity Calculations

Dilatational elasticity was calculated for different systems of $scCO_2$ and different aqueous phases. Figure 10 and Figure 11 show the elasticity of $scCO_2$ in contact with different aqueous solutions. It can be observed that adding PEI and PECNP to the surfactant solution increases the elasticity of the interface, which results in improving the foam stability.

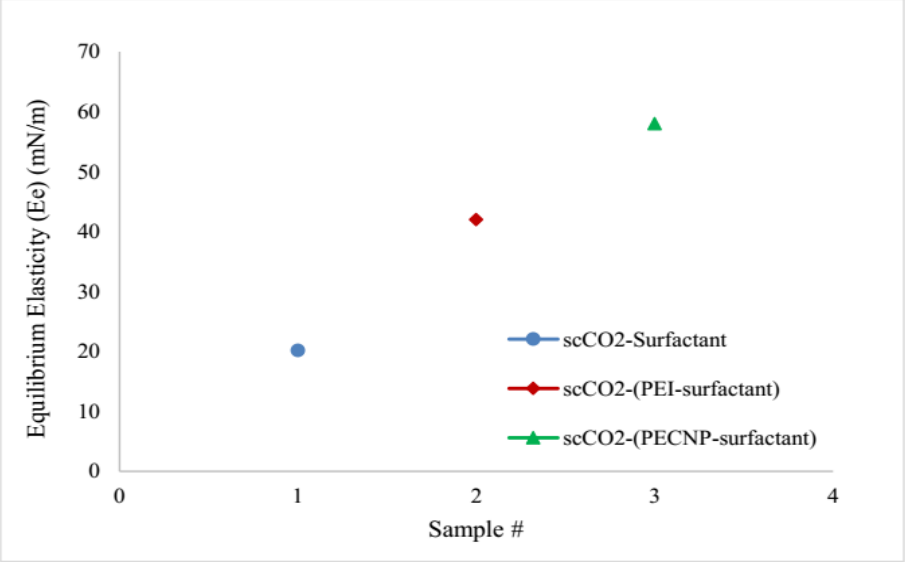

Figure 10. Equilibrium elasticity of different systems in 33,667 ppm salinity of diluted MLP brine.

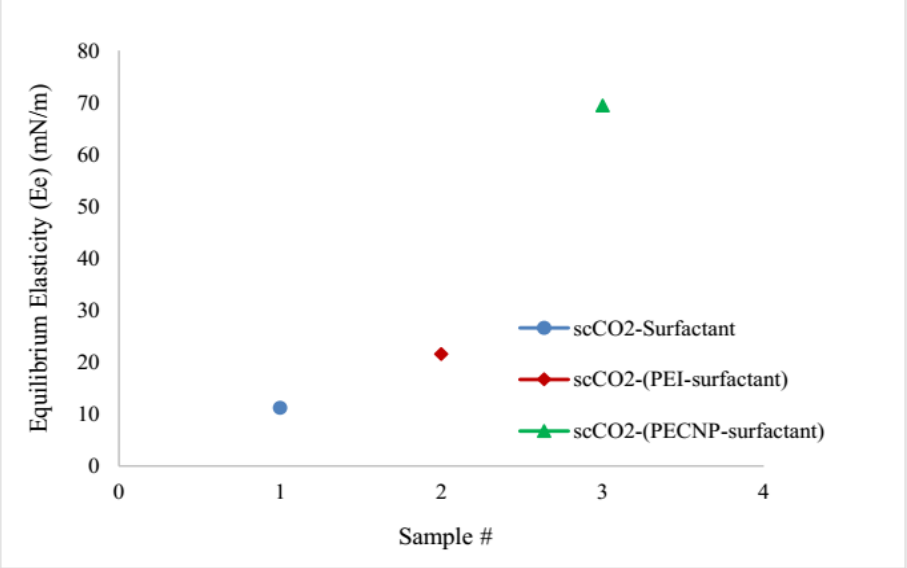

Figure 11. Equilibrium elasticity of different systems in 67,333 ppm salinity of diluted MLP brine.

Porosity and Permeability Measurement

In order to measure the permeability, the brine is flowed through the core holder in 3 different flow rates. A sample of the pressure drop versus time graph for different flow rates for permeability measurement is shown in Figure 12. The permeability measurement for core #2, as an example, is showed in Figure 13 and the slope of the plot is used to calculate the permeability using Darcy's Law and fluid and rock properties reported in Table 4. Table 5 shows the measured porosity and permeability for different cores used in different core flooding experiments with and without MLP crude oil in the system.

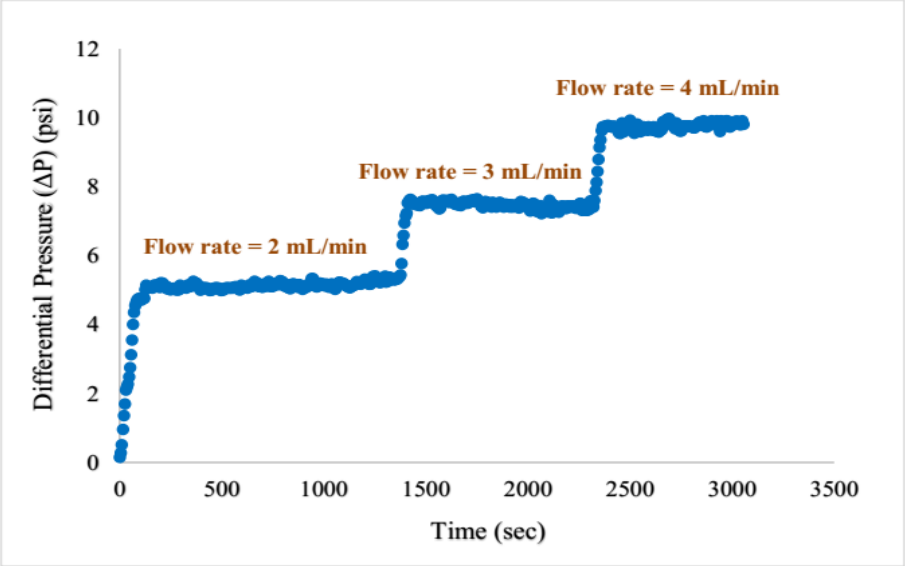

Figure 12. Pressure drop versus time graph for permeability calculation of the 9-inch Indiana limestone core. This plot belongs to core #17 given in Table 5.

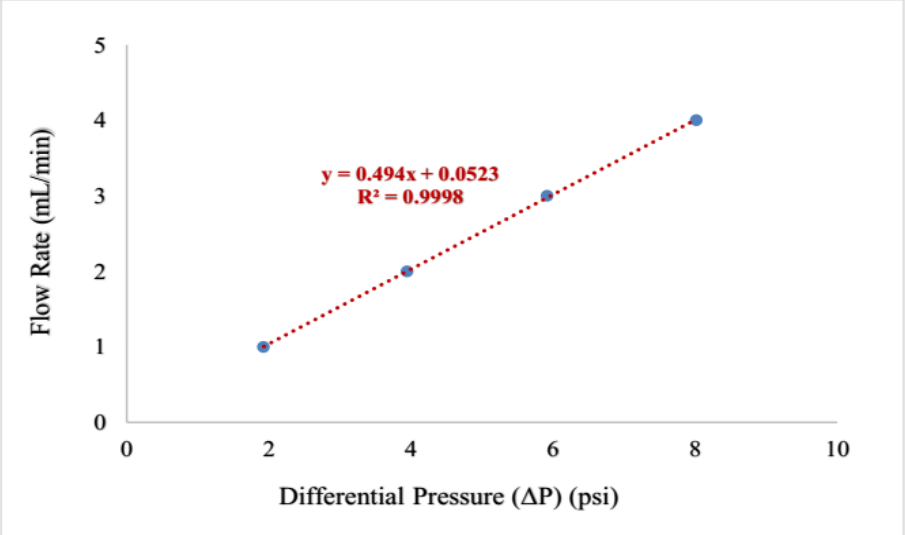

Figure 13. Flow rate versus pressure drop graph for permeability calculation of the 9-inches Indiana limestone core without the crude oil. This plot belongs to core #2 with the rock and fluid properties given in Table 4.

Table 4. The rock and fluid properties used for permeability calculations of core #2.

μ (cP)	L (cm)	r (cm)	A (cm^2)
0.75 or 0.8	22.86	3.81	11.4

Table 5. Summary of the measured permeability for the Indiana limestone cores used for the core flooding experiments with and without MLP crude oil.

Core #	Liquid used for Permeability Measurement	Bulk Volume (mL)	Pore Volume (mL)	Porosity (%)	Permeability (mD)
These 6 cores are used in core flooding experiments without oil.					
1	MLP 33,667	260.625	49.136	0.189	156.50
2	MLP 33,668	260.625	48.389	0.186	185.63
7	MLP 33,669	260.625	44.303	0.17	92.79
4	MLP 67,333	260.625	46.169	0.177	191.61
8	MLP 67,334	260.625	45.785	0.176	77.47
9	MLP 67,335	260.625	47.816	0.183	125.52
These 6 cores are used in core flooding experiments with oil.					
17	MLP 33,667	260.625	45.059	0.173	150.32
11	MLP 33,668	260.625	45.098	0.173	195.63
19	MLP 33,669	253.7	44.028	0.174	91.74
13	MLP 67,333	260.625	46.494	0.178	127.02
15	MLP 67,334	260.625	47.059	0.181	170.45
18	MLP 67,335	260.625	47.567	0.183	181.86

Foam Flooding in the Absence of Crude Oil

After measuring the permeability of the cores, they are flooded with two pore volumes of different aqueous phase solution. Thereafter, the cores are flooded with the CO_2 foam generated by the desired aqueous solution. The differential pressure generated by different systems of surfactant generated CO_2 foam, PEI-surfactant generated CO_2 foam, and PECNP-surfactant generated CO_2 foam for two different salinities of 33,667 and 67,333 ppm brine are shown in Figure 14 and Figure 15, respectively. It is noticed that adding polyelectrolytes and polyelectrolyte complex nanoparticles to the surfactant solution increases the differential pressure across the core and results in improving the apparent viscosity and stabilizing the foam front.

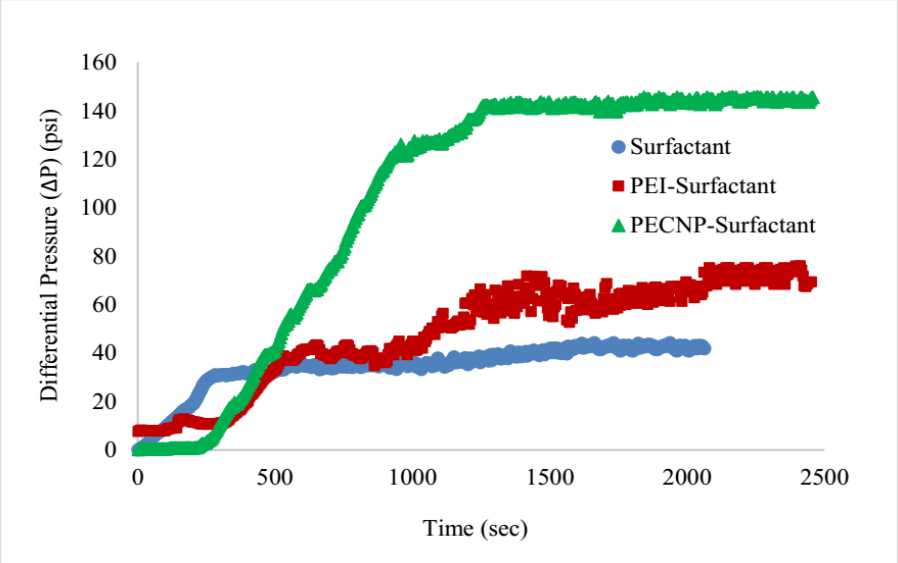

Figure 14. Differential pressure versus time for three different systems of surfactant, PEI-surfactant, and PECNP-surfactant generated CO_2 foams in 33,666 ppm salinity of diluted MLP brine.

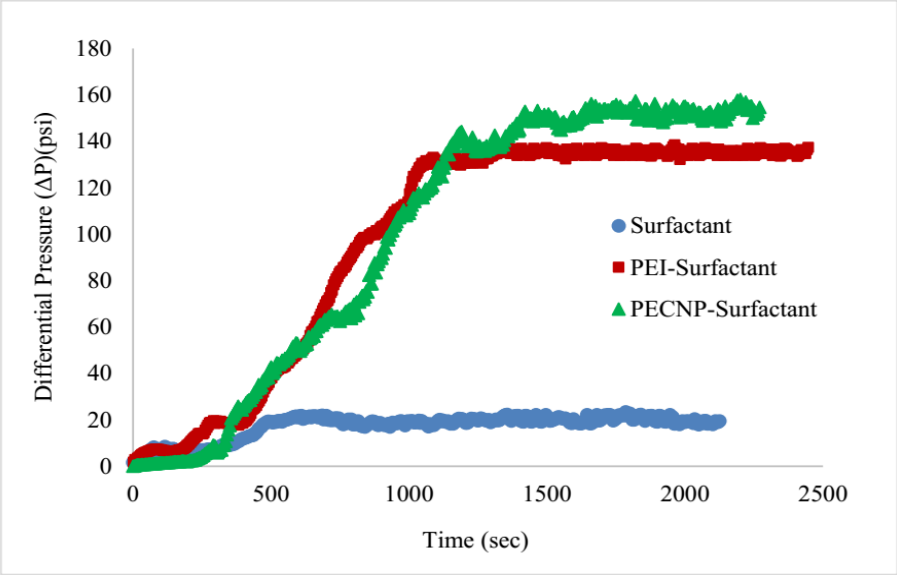

Figure 15. Differential pressure versus time for three different systems of surfactant, PEI-surfactant, and PECNP-surfactant generated CO_2 foams in 67,333 ppm salinity of diluted MLP brine.

Core Flooding Tests in the Presence of the MLP Crude Oil

The CO_2 foam improves the mobility control problems associated to CO_2 flooding. After studying the foam properties by different tests, the core flooding tests in the presence of crude oil are designed to analyze the oil production under different injection fluid types. The oil recovery under each injection scenario is calculated and the results are shown in Table 6 and
Table 7 for two different brine salinities of 33,667 and 67,333 ppm, respectively. The oil recovery for each core under different scenarios of injection are shown in Figure 16 through Figure 21. Comparison of the oil recovery for all the systems is discussed in the following sections.

Oil Recovery Discussion

Considering different scenarios of injection in Table 6 and
Table 7, the same scenario of injection is used for core #17 and #13, but in two different diluted MLP brine salinities of 33,667 ppm and 67,333 ppm. In core #17, the surfactant generated CO_2 foam flooding recovers 45.33% of the residual oil after water flooding. After injecting around 2.5 PV of the surfactant generated CO_2 foam, no more oil is produced by continuing the injection of surfactant generated CO_2 foam. The core is flooded with different systems of generated foams after the surfactant generated CO_2 foam flooding. By injecting 2.5 PV of the PECNP-surfactant generated CO_2 foam, 10.00% of the residual oil in the core after the surfactant flooding is produced. Injecting the PEI-surfactant generated CO_2 foam after the PECNP-surfactant generated foam injection does not produce any extra oil in 33,667 ppm salinity of the diluted MLP brine considering that the error of reading for the oil volume is 0.02 of the oil saturation. In the same procedure on core #13, injecting the surfactant generated CO_2 foam after water flooding produces 46.60 % of the residual oil in place and then when this foam is not productive after 2.5 PV of injection, injecting the PECNP-surfactant generated CO_2 foam, produces 10.75% of the residual oil in place after the surfactant foam flooding. Injecting the PEI-surfactant generated CO_2 foam after the PECNP-surfactant foam flooding recovers 4.38% of the residual oil in place after PECNP-surfactant foam flooding in 67,333 ppm salinity of diluted MLP brine. By changing the order of injection for different foam systems, the results are presented for cores #12 and #18 for two different salinities of 33,667 and 67,333 ppm salinities of diluted MLP brine. In both of them, the core is flooded with the PECNP-surfactant generated CO_2 foam after water flooding. In core #19, injecting the PECNP-surfactant generated CO_2 foam after water flooding results in recovering 54.35% of the residual oil in place after water flooding. In core #18, injecting the PECNP-surfactant generated CO_2 foam after water flooding, results in recovering

47.71% of the residual oil in place. Injecting the PEI-surfactant generated CO_2 foam after injecting 2.5 PV of the PECNP-surfactant generated CO_2 foam, results in recovering 20.46% of the residual oil in place for core #19 and 13.82% of the residual oil in place for core #18. The foam injection is continued by injecting the surfactant generated CO_2 foam after 2.5 PV of the PEI-surfactant generated CO_2 foam injection. Injecting 2.5 PV of the surfactant generated CO_2 foam recovers 2.34% of the residual oil in place for core #19 and 8.02% of the residual oil in place for core #18. Finally, in the last scenario, the core #11 and #15 are subjected to the same order of injection but in two different salinities of 33,667 ppm and 67,333 ppm salinities of diluted MLP brine. In the first step, the core is flooded with the PEI-surfactant generated CO_2 foam. Injecting the PEI-surfactant generated CO_2 foam results in recovering 32.45% of the residual oil in core #11 and 39.20% of the residual oil in core #15. After 2.5 PV of foam injection, there is not any oil production due to the PEI-surfactant generated CO_2 foam injection through the core. Therefore, the PEI foam injection is stopped and the cores are flooded with the PECNP-surfactant generated CO_2 foam. Injecting 2.5 PV of PECNP-surfactant generated CO_2 foam, recovers 8.58% of the residual oil in core #11 and 10.08% of the residual oil in core #15. The foam injection continues by injecting the surfactant generated CO_2 foam through the cores. 6.57% of the residual oil in core #11 and 1.12% of the residual oil in core #15 is recovered due to injecting 2.5 PV of the surfactant generated CO_2 foam in the cores.

By looking at the recovery factor and the residual oil saturation values in Table 6 and

Table *7*, it is observed that the second scenario gives the highest recovery after the water flooding for both salinities of 6 and 3 times diluted MLP brine. Therefore, applying this scenario of injection (surfactant generated CO_2 foam followed by PECNP-surfactant generated CO_2 foam), for the production wells which are water flooded, results in the highest amount of the oil production and the highest values of recovery factor. The first scenario can be considered for the oil wells which have been surfactant foam flooded and there is not any extra oil recovery due to the surfactant generated CO_2 foam injection. In this scenario, injecting the PECNP-surfactant generated CO_2 foam after surfactant foam flooding recovers 10% of the residual oil in place after the surfactant generated CO_2 foam flooding. This is due to the improved stability of the nanoparticles generated CO_2 foams in the presence of crude oil. Polyelectrolyte complex nanoparticles by stabilizing the interface because of the electrostatic forces, prevent surfactants from leaving the interface and therefore, stabilize the generated foams in the presence of crude oil even in high salinity reservoirs. PEI give the interfaces a stronger charge and therefore making them more stable. These effects are coupled with the improvement effect of PECNPs on the viscosity of the aqueous phase.

Table 6. Summary of the oil saturation and oil recovery percentage after each system of foam injection in 33,667 ppm salinity of diluted MLP brine. Note that the percentages are based on the oil in place at the end of the previous flood. The numbers with a * sign is neglected based on the error limits.

System	Oil Saturation	Recovered Oil (%)
Core # 17		
After Primary Drainage	0.612	
After Waterflooding	0.284	53.58
After surfactant generated CO_2 foam	0.155	45.33
After PECNP-surfactant generated CO_2 foam	0.140	10.00
After PEI-surfactant generated CO_2 foam	0.139*	0.80
Core # 19		
After Primary Drainage	0.512	
After Waterflooding	0.267	47.76
After PECNP-surfactant generated CO_2 foam	0.122	54.35

After PEI-surfactant generated CO_2 foam	0.097	20.46
After surfactant generated CO_2 foam	0.095*	2.34
Core # 11		
After Primary Drainage	0.715	
After Waterflooding	0.383	46.45
After PEI-surfactant generated CO_2 foam	0.259	32.45
After PECNP-surfactant generated CO_2 foam	0.236	8.58
After surfactant generated CO_2 foam	0.221*	6.57

Table 7. Summary of the oil saturation and oil recovery percentage after each system of foam injection in 67,333 ppm salinity of diluted MLP brine. Note that the percentages are based on the oil in place at the end of the previous flood. The numbers with a * sign is neglected based on the error limits.

System	Oil Saturation	Recovered Oil (%)
Core # 13		
After Primary Drainage	0.654	
After Waterflooding	0.350	46.60
After surfactant generated CO_2 foam	0.220	36.96
After PECNP-surfactant generated CO_2 foam	0.196	10.75
After PEI-surfactant generated CO_2 foam	0.188*	4.38
Core # 18		
After Primary Drainage	0.540	
After Waterflooding	0.291	46.17
After PECNP-surfactant generated CO_2 foam	0.152	47.71
After PEI-surfactant generated CO_2 foam	0.131	13.82
After surfactant generated CO_2 foam	0.123*	8.02
Core # 15		
After Primary Drainage	0.648	
After Waterflooding	0.350	45.93
After PEI-surfactant generated CO_2 foam	0.213	39.20
After PECNP-surfactant generated CO_2 foam	0.192	10.08
After surfactant generated CO_2 foam	0.190*	1.12

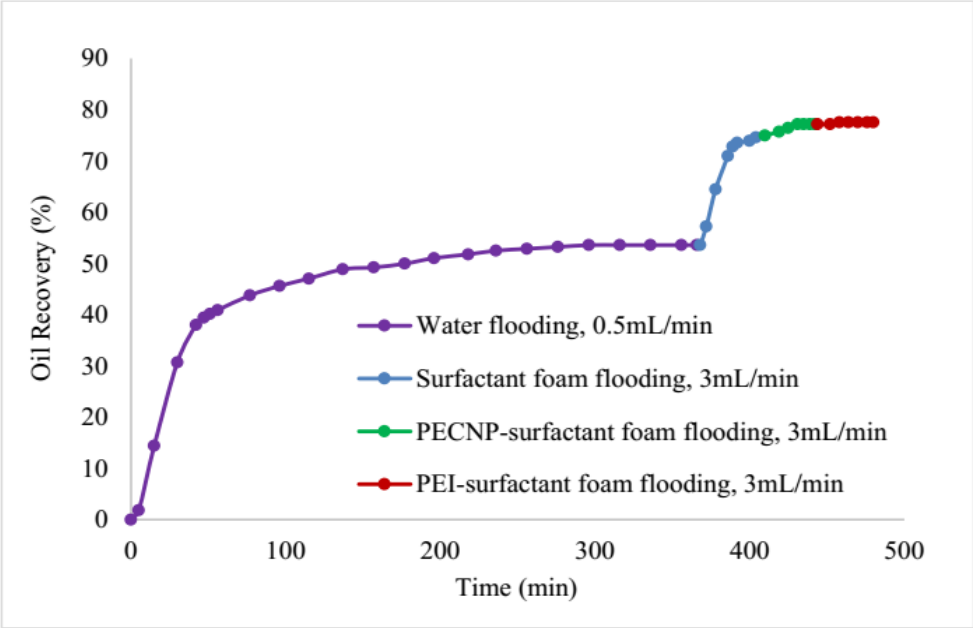

Figure 16. Oil production versus time for different foam injections in core #17 in 33,667 ppm salinity of diluted MLP brine.

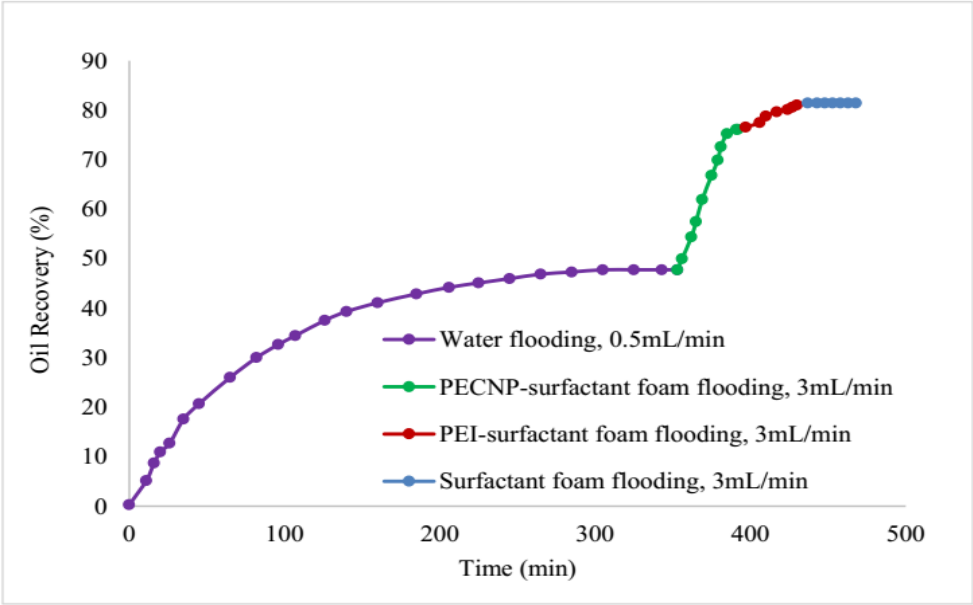

Figure 17. Oil production versus time for different foam injections in core #19 in 33,667 ppm salinity of diluted MLP brine.

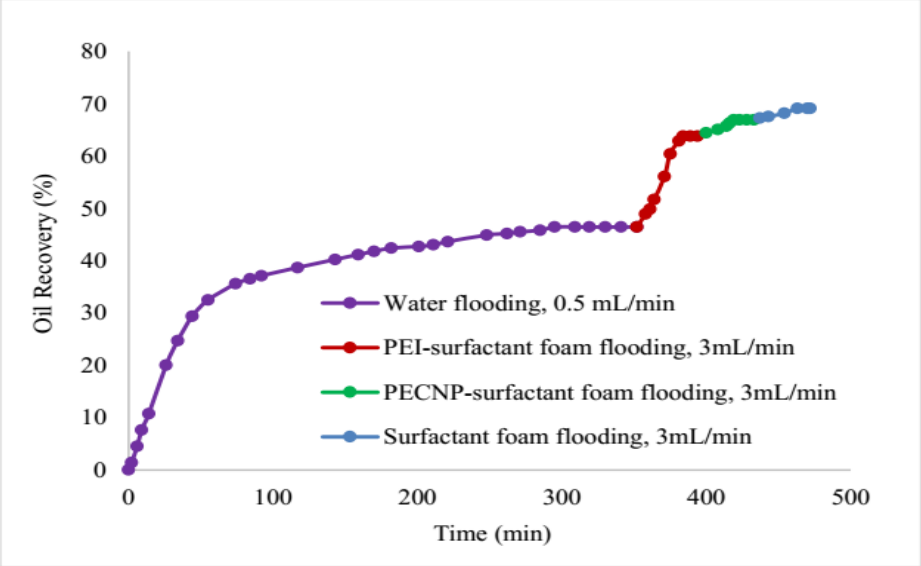

Figure 18. Oil production versus time for different foam injections in core #11 in 33,667 ppm salinity of diluted MLP brine.

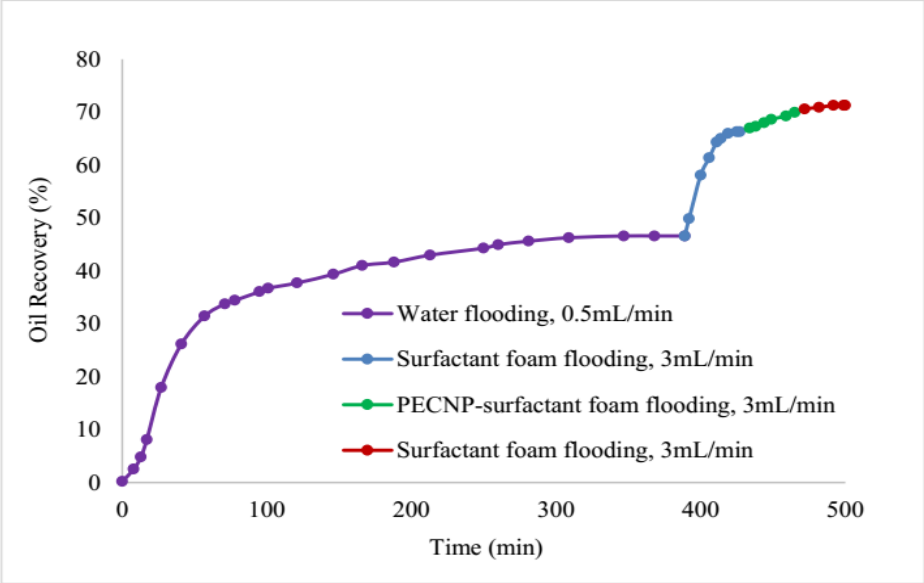

Figure 19. Oil production versus time for different foam injections in core #13 in 67,333 ppm salinity of diluted MLP brine.

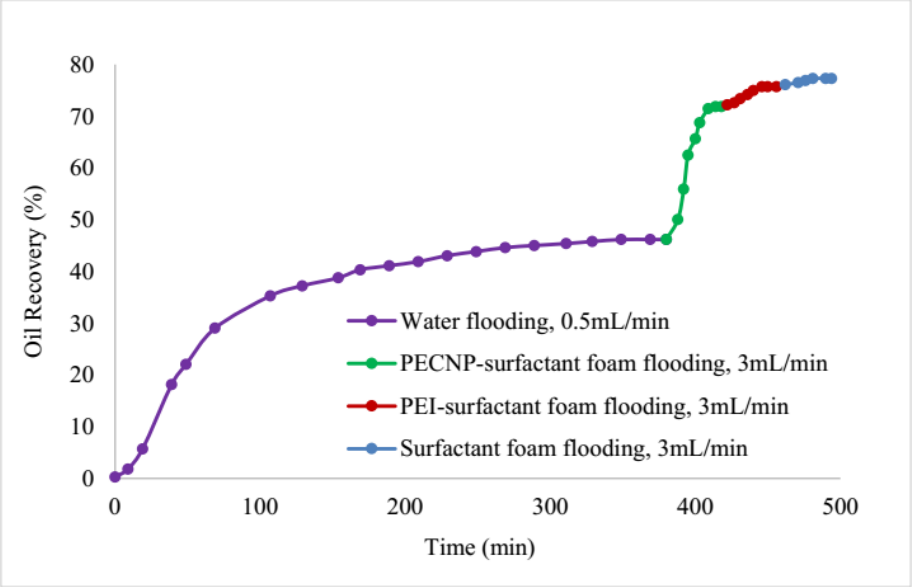

Figure 20. Oil production versus time for different foam injections in core #18 in 67,333 ppm salinity of diluted MLP brine.

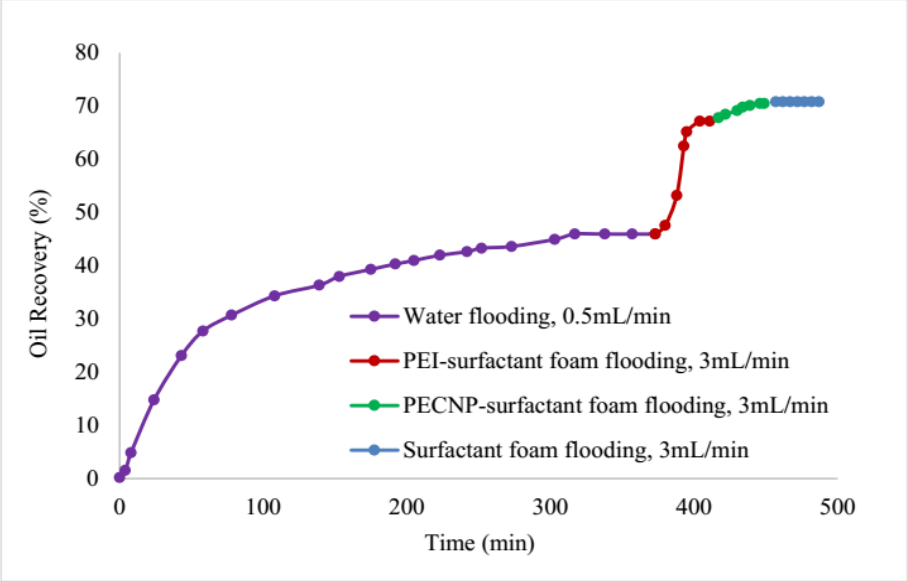

Figure 21. Oil production versus time for different foam injections in core #15 in 67,333 ppm salinity of diluted MLP brine.

Conclusions

Polyelectrolytes and polyelectrolyte complex nanoparticles have successfully improved the oil recovery when tested at reservoir conditions and prepared using high salinity brine.

1) Adding polyelectrolytes and polyelectrolyte complex nanoparticles to the surfactant solution results in decreasing the dynamic interfacial tension between oil and water. Decreasing IFT results in improving the enhanced oil recovery.
2) Comparing the surface dilatational elasticity measurements shows that adding PEI and PECNP to the surfactant solution led to a higher surface dilatational elasticity. Increasing the surface elasticity results in improving the surface viscosity and higher lifetime of the generated foam. Increasing the foam lifetime improves the efficiency of the enhanced oil recovery mechanism.
3) Different systems of foam including surfactant generated CO_2 foam, PEI-surfactant generated CO_2 foam, and PECNP-surfactant generated CO_2 foam were injected into the core. It was observed that the PECNP-surfactant generated CO_2 foam showed the highest pressure drop and hence

corresponding to the highest average effective viscosity followed by the PEI- surfactant foam in both salinities of 33,667 and 67,333 ppm. The obtained results from the core flooding experiments without the crude oil in the system can be interpreted as the stable nature of the system for oil recovery applications.

4) Improving the oil recovery efficiency even by a few percent is the goal of all enhanced oil recovery techniques. Different systems of surfactant generated CO_2 foam, PEI-surfactant generated CO_2 foam, and PECNP-surfactant generated CO_2 foam were injected into the different core plugs after the water flooding process. It was observed that the oil recovery achieved by injecting the PECNP-surfactant generated CO_2 foam after waterflooding was higher, by 10-11%, than injecting the surfactant generated CO_2 foam alone in the reservoirs up to 67,000 ppm of salinity. In addition, injecting the PECNP- surfactant generated CO_2 foam can be considered for the oil wells which have been surfactant foam flooded without any extra oil recovery. It was proven that injecting the PECNP-surfactant generated CO_2 foam after surfactant foam flooding recovers 10% of the residual oil in place. This is due to the stability of the nanoparticle generated CO_2 foams in the presence of crude oil. Polyelectrolyte complex nanoparticles, by stabilizing the interface, because of the electrostatic forces, and improving the viscosity of the lamellae, prevent surfactants from leaving the interface and therefore, stabilize the generated foams in the presence of crude oil even in high salinity reservoirs.

Acknowledgements

This project is partially funded by the National Science Foundation EPSCoR Research Infrastructure Improvement Program: Track -2 Focused EPSCoR Collaboration award (OIA- 1632892). The authors would like to extend their appreciation to Kansas Interdisciplinary Carbonates Consortium (KICC) for partially funding this project. We would also like to extend our appreciation to Huntsman Chemicals Inc. for providing the surfactant used for this study. Authors would like to thank Mr. Zach Kessler rom the Chemical and Petroleum Engineering department and Mr. Scott Ramskill from the Tertiary Oil Recovery Program (TORP) at the University of Kansas for their kindly helps for installing and maintaining the lab equipment.

Nomenclature

π: Surface pressure
E: Dilatational elasticity
t: Time of compression (s)
τ: Time of relaxation (s)
A: Surface area (cm^2)
k: Permeability (mD)
μ: Viscosity (cP)
L: Length (cm)
P: Pressure (atm)
Q: Flow rate (cm^3/s)

References

Barati, R., December 2010. *Fracturing Fluid Cleanup by Controlled Release of Enzymes from Polyelectrolyte Complex Nanoparticles,* Lawrence, KS: University of Kansas.

Barati, R., Pennel, S., Matson, M. & Linroth, M., 2016. *Overview of CO_2 Injection and WAG Sensitivity in SACROC.* Tulsa, OK, SPE.

Bernard, G. G. & Holm, L. W., 1967. *Method for Recovering Oil from Subterranean Formations, U. S. Patent 3,342,256,* Grant: Patent.

Boury, F. et al., 1995. Dilatational Properties of Adsorbed Poly(D,L-lactide) and Bovine Serum Albumin Monolayers at the Dichloromethane/Water Interface. *Langmuir,* 11(5), p. 1636–1644.

Caudle, B. & Dyes, A., 1958. Improving Miscible Displacement by Gas-Water Injection. *SPE, American Invitational Mathematics Examinations (AIME),* pp. 213, 281.

Caudle, D. D., 2002. *Produced Water Regulations in United States: Then, Now and in the Future.* San Antonio, TX, SPE.

Evans, P. & Robinson, K., 1999. *Produced Water Management-Reservoir and Facilities Engineering Aspects.* Bahrain, SPE.

Fried, A., 1961. *The Foam-Drive Process for Increasing the Recovery of Oil,* Washington D. C., USA: Report of Investigation 5866, USBM.

Green, D. & Willhite, P., 1998. *Enhanced Oil Recovery.* Richardson, TX: Society of Petroleum Engineers (SPE).

JPT, 1998. CO_2 Foam Floods: Foam Properties and Mobility Reduction Effectiveness. *Society of Petroleum Engineers (SPE), JPT Journal*.

Kalyanaraman, N. et al., 2016. Stability improvement of CO_2 foam for enhanced oil-recovery applications using polyelectrolytes and polyelectrolyte complex nanoparticles. *Journal of Applied Polymer Science,* 134(6).

Kristen, N. & Klitzing, R. V., 2009. Effect of Polyelectrolyte/Surfactant Combinations on the Stability of Foam Films. *Soft Matter,* 6(2010), pp. 849-861.

Langston, M. V., Hoadley, S. F. & Young, D. N., 1988. Definitive CO_2 Flooding Response in the SACROC Unit. *SPE, Enhanced Oil Recovery.*

Lord, D. L., 1981. Analysis of Dynamic and Static Foam Behavior. *Society of Petroleum Engineers (SPE), JPT Journal*, January, pp. 39-45.

Micheau, C., Bauduin, P., Diat, O. & Faure, S., June 2013. Specific Salt and pH Effects on Foam Film of a pH Sensitive Surfactant. *Langmuir, American Chemical Society (ACS),* 29(27), p. 8472–8481.

Nazari, N., Tsau, J. S. & Barati, R., 2017. CO_2 Foam Stability Improvement Using Polyelectrolyte Complex Nanoparticles in Produced Water. *Journal of Energies,* 10(4).

Patel, C., Barrufet, M. A. & Petriciolet, A. B., 2004. *Effective Resource Management of Produced Water in Oil and Gas Operations.* Alberta, Canada, 5th Canadian International Petroleum Conference.

Schramm, L. L., 1994. Foam Sensitivity to Crude Oil in Porous Media. In: *Foams, Fundamentals and Applications in the Petroleum Industry.* Washington, DC: American Chemical Society, pp. 165-197.

Sedev, R. & Exerowa, D., 1999. DLVO and Non-DLVO Surface Forces. *Advance Colloid Interface Science,* Volume 83, pp. 111-136.

Tewes, F., Pierre Krafft, M. & Boury, F., 2011. Dynamical and Rheological Properties of Fluorinated Surfactant Films Adsorbed at the Pressurized CO_2–H_2O Interface. *Langmuir,* 27(13), p. 8144–8152.

Xu, W., 2005. *Experimental Investigation of Dynamic Interfacial Interactions at Reservoir Conditions,* Louisiana State University: Thesis.

Yemul, O. & Imae, T., June 2008. Synthesis and Characterization of Poly(ethyleneimine) Dendrimers. *Colloid and Polymer Science,* 286(6), p. 747–752.